Journal of Electroceramics, 10, 103–110, 2003

Structural and Dielectric Characterization of Sol-Gel Fabricated $PbTiO_3$ Thin Films Doped with Lanthanide Ions

S. IAKOVLEV, C.-H. SOLTERBECK & M. ES-SOUNI*

University of Applied Sciences, Institute for Materials and Surface Technology (IMST), Grenzstrasse 3, 24149 Kiel, Germany

Submitted April 8, 2003; Revised May 28, 2003; Accepted May 29, 2003

Abstract. Lanthanide elements doped $PbTiO_3$ thin films were prepared by a modified sol-gel method via spin-coating on platinized silicon substrates. The films microstructure and phase composition were investigated by means of scanning electron microscopy, X-ray diffractometry and Raman spectroscopy. Small signal dielectric properties of the films were characterized at different temperatures and doping element concentration. It is shown that dielectric constant, loss tangent and Curie transition temperature of lanthanide elements doped thin films correlate with concentration and ionic radii of these elements. The results obtained are discussed from the point of view of substitution type and compared to some extent to the data, reported by other research groups.

Keywords: sol-gel method, $PbTiO_3$, dielectric properties, Curie temperature, cation substitution, lanthanide elements

1. Introduction

$PbTiO_3$ (PT) based ferroelectric thin films exhibit unique dielectric, piezoelectric and ferroelectric properties which make them attractive for many technological applications such as in micro-electromechanical systems (MEMS) [1], non-volatile memories [2], infrared (IR) sensors [3, 4], etc. Dielectric and pyroelectric properties of the films may be tuned for specific application by appropriate doping. Analysis of the literature shows that among doping elements La [5–11] was the most investigated element. The behaviour of other elements of the lanthanide series has been investigated systematically mainly in bulk ceramics. Park et al. [12] prepared and investigated 3 mol% of La, Nd, Sm, Gd, Dy, Ho, Er, and Yb (Ln in the following) doped PLZT (lead lanthanum zirconate titanate) ceramics. Structure and properties of PZT (lead zirconate titanate) ceramics with respect to ionic radii of rare-earth elements were reported by Tan et al. [13] and Sharma et al. [14]. Properties of La, Sm and Er modified PZT ceramics were also reported by Pramila et al. [15], and Shannigrahi et al. [16]. The data on the lanthanide elements doping effects in PZT ceramics can also be found in textbooks (see, for example Ref. [17]). Structure and properties of rare-earth ions doped ferroelectric thin films are studied to lesser degree and the data are scarce. Boyle et al. [18] have reported the effect of 4 mol% of Ln doping on the structure, dielectric and ferroelectric properties of PZT thin films with the composition PLnZT (4/30/70). Furthermore, investigation of Ln doping on $PbTiO_3$ thin films are still lacking. In a recent work we report on the optical properties (refractive index and extinction coefficient) of Ce, Sm, Dy, Er, and Yb doped $PbTiO_3$ thin films in comparison to non-doped one [19]. The results of the optical characterization demonstrate that the refractive index and extinction coefficient depend not only on the concentration of lanthanide ions but are also sensitive to atomic number/ionic radii and oxidation state of dopant. In the present paper emphasis is put on the effects of rare-earth elements doping on the structure and dielectric properties of $PbTiO_3$ thin films. Ce, Sm, Dy and Er doped lead titanate thin films were deposited via a modified sol-gel method on platinized silicon substrates. The results are analysed in terms of effects of doping on dielectric constant and loss tangent as well as transition temperature, and

*To whom all correspondence should be addressed. E-mail: mohammed.es-souni@fh-kiel.de

compared to those reported on PZT ceramics and thin films.

2. Experimental

Acetic acid, acetylacetone and 2-methoxyethanol based sol-gel method was utilized to fabricate lanthanide series elements doped lead titanate thin films with different doping levels. The flow chart diagram on Fig. 1 illustrates the process of precursor solutions preparation. Lead acetate, tetraisopropyl orthotitanate, acetic acid, acetylacetone and 2-methoxyethanol were provided by Fluka Chemical, Inc., Germany. Ce, Sm, Dy and Er acetates were purchased from Strem Chemicals, Inc., U.S.A. 10 mol% of Pb excess were added solution to compensate lead volatility at the subsequent high temperature treatment. $Pb_{(1-x)1.1}Ln_xTiO_3$ stoichiometric composition was chosen to calculate the amount of reagents. 2, 5 and 8 mol% ($x = 0.02$, 0.05 and 0.08) of Ln were designated to replace lead. Firstly lead and Ln acetates were dissolved in acetic acid and refluxed for 3 hours at 110°C to evaporate associated water. 3 mols of acetic acid were taken to dissolve 1 mol of lead and Ln acetates. Tetraisopropyl orthotitanate was stabilized with acetylacetone in ratio 1:2 mol. Both parts were then mixed together at room temperature and diluted with 2-methoxyethanol to reach final concentration of 0.4 mol/l. Regardless of doping element and doping level yellow, transparent sols were obtained. The solutions were filtered through 0.2 μm syringe filter just prior to film deposition. The PLnT thin films were formed via spin-coating on (111)Pt/Ti/SiO_2/Si commercial substrates (Inostek, Seoul, Korea) at 3000 rpm for 30 s. 4 layers were deposited for each sample giving an ellipsometric thickness in the range from 200 to 300 nm. Each coating was dried on a plate at 340°C for 5 min and pyrolized at 550°C for 5 min in air. Finally, the samples were annealed in a pre-heated furnace at 700°C for 5 min.

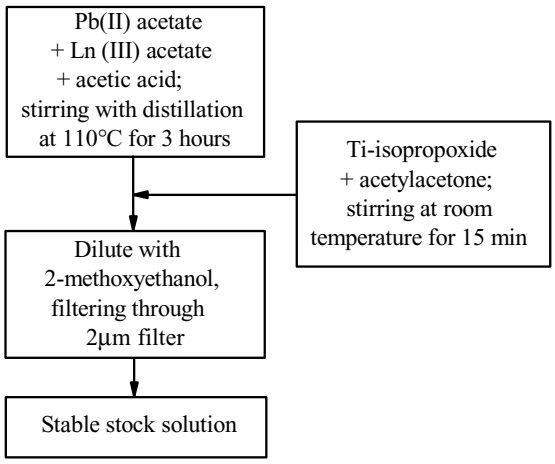

Fig. 1. Flow chart for lanthanide elements doped lead titanate precursor solution preparation.

Microstructure and phase composition of the films were characterized by means of scanning electron microscopy (SEM, Philips XL 30) and X-ray diffractometry (XRD, Seifert powder diffractometer, Cu K_α radiation, $\Theta/2\Theta$ scans, $2\Theta = 20$–50°). Dilor XY spectrometer, equipped with Ar-Kr laser was used for Raman characterization of pure and 2 mol% of Ln-elements doped samples. For electrical measurements, capacitors were fabricated by sputtering round Pt top electrodes of 0.6 mm diameter through a shadow mask. Post top electrode deposition annealing was conducted in air at 400°C for 15 min. Contact to the bottom electrode was produced by scratching a corner of the specimen and subsequent deposition of high purity silver paste. Small signal dielectric properties were measured using a computer controlled Agilent 4192A impedance analyser at driving signal amplitude of 50 $mV_{p\text{-}p}$. The temperature dependence of the dielectric properties was measured in the temperature range from 460°C to 23°C on cooling.

3. Experimental Results

3.1. Microstructure, X-Ray and Raman Characterization

The surface topography and grain morphology are exemplified in Fig. 2 which shows a back scattered electron (BSE) SEM micrograph of a pure $PbTiO_3$ thin film (a), and films doped with 2 mol% of Ce (b) and 8 mol% of Dy. One can see that the specimen preparation procedure described above leads to crack-free and uniform microstructure with a grain size less than 100 nm. The figures also show that doping with various elements of lanthanide series affects surface roughness rather than grain size. Although further surface characterization (for example, by means of the Scanning Probe Microscopy) is required.

Phase composition was examined by means of XRD analysis. Figure 3 illustrates the XRD pattern of

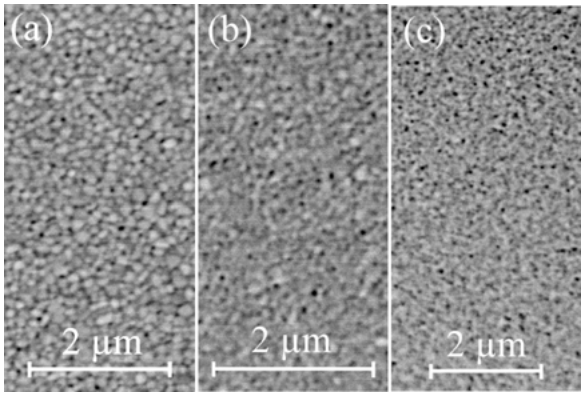

Fig. 2. Back-scattered electron SEM micrograph of pure lead titanate thin film (a), doped with 2 mol% of Ce (b) and 8 mol% of Dy (c).

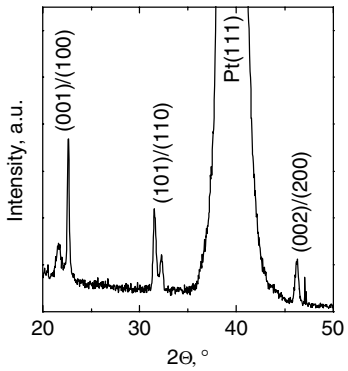

Fig. 3. XRD pattern of sol-gel fabricated lead titanate thin film.

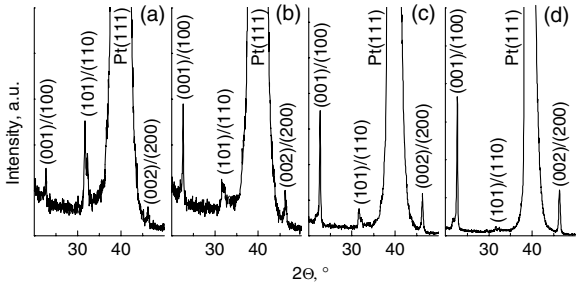

Fig. 4. XRD patterns of sol-gel fabricated lead titanate thin films, doped with 2 mol% of Ce (a), Sm (b), Dy (c) and Er (d).

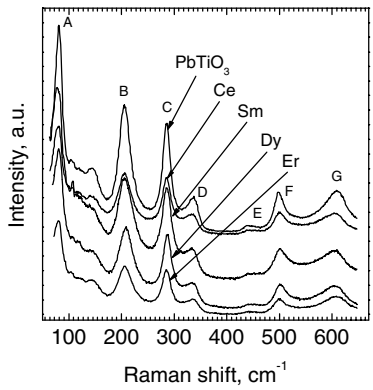

Fig. 5. Room temperature Raman spectra of pure $PbTiO_3$ and films doped with 2 mol% of Ln-elements lead titanate thin films. Raman modes are indicated by letters: A—E(1TO), B—A_1(1LO) + E(2TO), C—B_1 + E (silent), D—A_1(2TO), E—E(2LO) + A_1(2LO), F—E (3TO), G—A_1(3TO).

non-doped lead titanate thin film. Annealing at 700°C for 5 min leads to the formation of pure tetragonal perovskite phase with no second phase inclusion (within the resolution of the diffractometer). The most possible pyrochlore phase, which manifests itself with a broad peak in the vicinity of 30°, was not detected.

X-ray diffraction patterns obtained for films doped with 2 mol% of Ln elements are represented in Fig. 4. It can be seen that in the case of small concentration of Ce, Sm, Dy and Er (Fig. 4(a)–(d)) no phase modification occurs. With increasing doping level (not shown), Sm doped films show no second phase for all concentrations investigated, whereas the XRD spectra of the films doped with 8 mol% of Dy and Er contain broad peaks in the vicinity of 30° (2Θ) which is attributed to the (222) reflection of non-ferroelectric pyrochlore phase. The appearance of the pyrochlore phase in doped $PbTiO_3$ thin films with decreasing radii of dopant ions is in agreement with the results reported by Tan et al. [13], and is explained by lower solubility of the elements with smaller ionic radii in the perovskite phase.

Results of room temperature Raman characterization are given on Fig. 5 for the specimens doped with 2 mol% of Ln elements in comparison to pure $PbTiO_3$ film. The spectra are very similar to those reported by many research groups for PT and tetragonal PZT thin films deposited by different methods [20–22]. The results indicate that the films are well crystallized into the tetragonal perovskite phase. At first sight one can see that: (i) Raman modes are shifted to lower values of wave number with respect to data, known for single crystals [23]; (ii) the spectra obtained for doped specimens demonstrate somewhat broader peaks as to compare to those of pure $PbTiO_3$ sample; (iii) positions of Raman modes were not affected by doping.

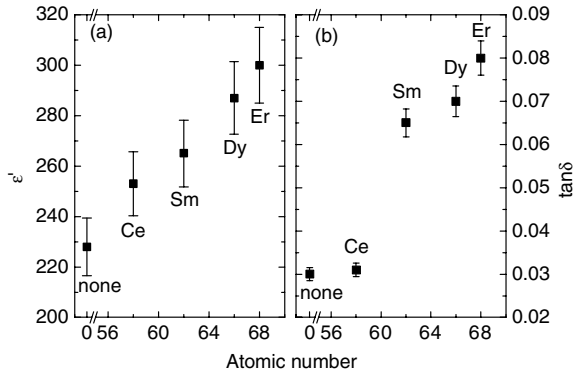

Fig. 6. Room temperature dielectric constant, ε' (a) and tanδ (b) of lead titanate thin films doped with 2 mol% of Ln-elements. Properties were measured with an AC signal of amplitude 50 $mV_{p\text{-}p}$ at 1 kHz.

3.2. Room Temperature Dielectric Properties

Figure 6 demonstrates how the dielectric properties (real part of the dielectric constant, ε' (Fig. 6(a)) and tanδ (Fig. 6(b)) of lead titanate thin films doped with 2 mol% of Ln ions correlate with atomic number. It can be seen that all doping elements lead to increase in both ε' and tanδ in comparison to non-doped lead titanate thin film. When atomic number of dopant increases from 58 (Ce) to 68 (Er), ε' and tanδ increase smoothly from 253 and 0.03 to the values of 300 and 0.08, respectively.

The dielectric properties of Ce, Sm, Dy and Er doped specimens are plotted vs. doping level, x, in Fig. 7. The error bars are not shown on the figure for simplicity. For doping element concentrations up to 5 mol% it can be noticed that ε' generally increases with increasing doping level. Higher concentrations lead for Sm and Er doped films to lower ε' whereas the values of Dy doped films continue to increase. Loss factor is found to increase in the case of Sm and Er doped samples for concentrations lower than 5 mol% and decrease for concentrations higher than 5 mol%. Yet Dy doping show maximum of tanδ at $x = 0.02$ (2 mol%).

3.3. Curie Phase Transition Temperature of Pure and Ln-Elements Doped Lead Titanate Films

The temperature dependence of the dielectric constant was found for all specimens to exhibit one maximum attributed to the corresponding Curie transition temperature, T_c. As an example Fig. 8 represents the

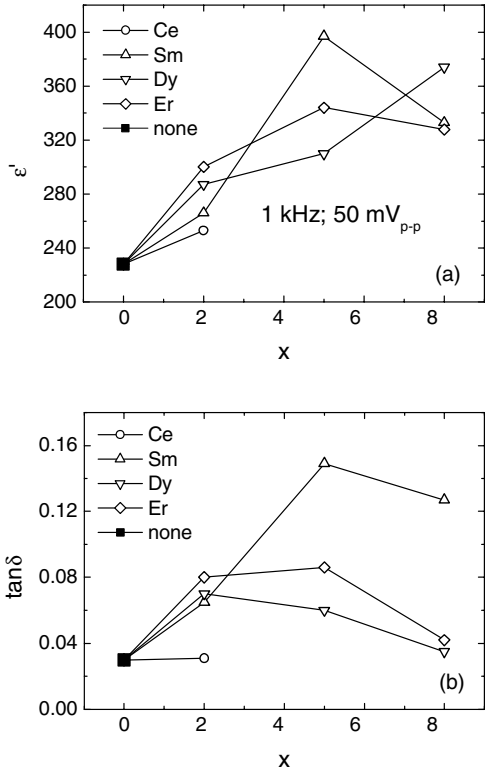

Fig. 7. ε' (a) and tanδ (b) of lead titanate thin films doped with Ce, Sm, Dy and Er, plotted vs. doping level, x (given in mol%).

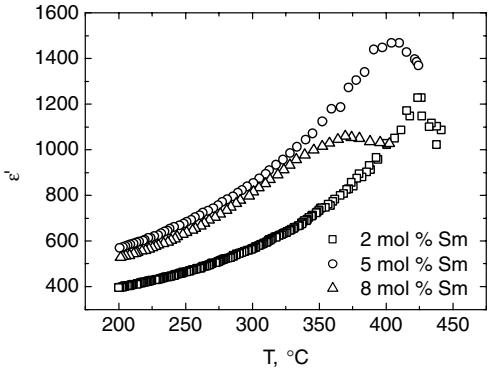

Fig. 8. Temperature dependence of dielectric constant acquired for lead titanate thin films doped with 2, 5 and 8 mol% of Sm. Measurements were done on cooling with the frequency of AC signal 1 kHz and the amplitude 50 $mV_{p\text{-}p}$.

temperature dependence a acquired at fixed frequency (1 kHz) on cooling for set of specimens including 2, 5 and 8 mol% of Sm doped lead titanate thin films. The values of T_c were also obtained at different frequencies for all prepared specimens. No frequency dependence

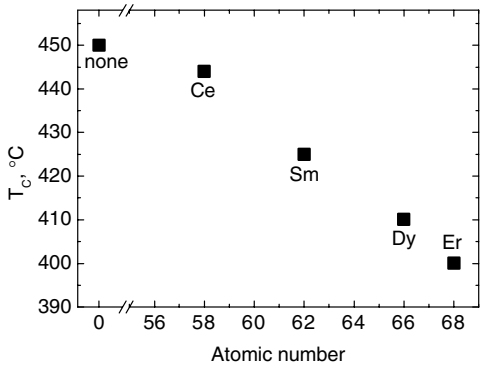

Fig. 9. Ferroelectric-paraelectric phase transition temperature of $PbTiO_3$ thin films doped with 2 mol% of lanthanide ions. The results are given in comparison to non-doped specimen.

of T_c was found (nonrelaxor-type) for all doping elements and concentrations. Figure 9 shows that T_c correlates with the atomic number of doping elements. It must be stressed firstly that the non-doped $PbTiO_3$ thin film (Fig. 9) revealed paraelectric-to-ferroelectric phase transition at a much lower temperature than that reported for bulk specimen (compare $T_c(PbTiO_3$ ceramics) = 490°C [p. 12 in Ref. 17] vs. 450°C, found for our film). Doping is found to decrease the ferroelectric transition temperature. Generally a smooth decrease of T_c with increasing atomic number is obtained. It is important to note that in the case of low doping level (here 2 mol%) Curie transition temperature is found to be more sensitive parameter to the atomic number/ionic radii of doping ions than the position of soft mode, responsible for paraelectric-ferroelectric phase transition in lead titanate. The dependence of T_c on doping level is shown in Fig. 10. A continuous decrease in

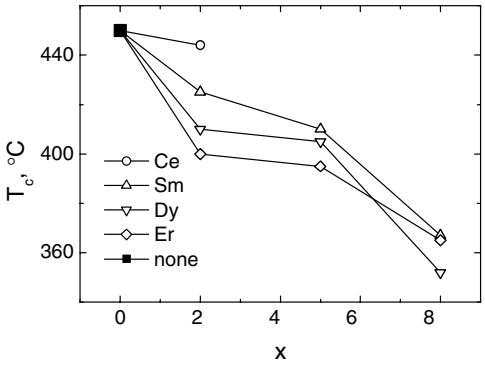

Fig. 10. Curie temperature of Ce, Sm, Dy and Er doped $PbTiO_3$ thin films plotted vs. doping level.

T_c can be seen for the doping elements Ce, Sm, Dy, and Er.

4. Discussion

4.1. X-Ray Diffractometry and Raman Spectroscopy of Pure and Ln-Elements Doped $PbTiO_3$ Thin Films

The main problem of X-ray diffractometry of PT based thin films deposited on platinized substrates lies in the fact that the (111) reflection overlaps with the intense (111) reflection from textured platinum electrode in the vicinity of $2\theta = 40°$. This limitation does not allow having an exact idea about the ratio of peak intensities, i.e. about preferential orientation of the films. Thereby only the ratio of (001)/(100) and (101)/(110) main peaks can be discussed. From Fig. 3 we can see that the ratio of (001)/(100) to (101)/(110) (R) peak intensities differs qualitatively from that, obtained for lead titanate powder [24], where the most intense peaks are (101)/(110).

It seems that depending on the concentration and nature of doping ions, thin film may be to some extent preferentially oriented or, otherwise, randomly crystallized. Figure 4 represents XRD patterns of 2 mol% of Ce, Sm, Dy and Er doped lead titanate thin films. The film doped with 2 mol% of Ce reveals lower R than for pure PT (more intense (101)/(110) peaks). Yet for Sm, Dy and Er doped specimens (Fig. 4(b)–(d)) the (101)/(110) peaks are largely attenuated. Furthermore, modification of lead titanate thin films with Sm, Dy and Er with concentrations higher than 5 mol% leads to complete suppression of (101)/(110) reflections, i.e. Sm, Dy and Er doping promotes rather textured state of the specimens. Another important feature is that in the case of doped films splitting of (001)/(100), (101)/(110) and (002)/(200) peaks is no longer observed (compare Figs. 3 and 4(a)–(d)). Explanation may be found in the promotion of a high degree of a- or c- domains in doped specimens [25].

The Raman spectra of lead titanate thin films contain all the features peculiar to that of single crystal $PbTiO_3$. It is known that Raman spectrum obtained for thin films is affected by physical state of the films [20–22]. Shift of Raman lines towards lower values of wave number (compare for example positions of E(1TO) soft mode 89 cm^{-1}, known for $PbTiO_3$ crystal [23] with 81 cm^{-1} found for our $PbTiO_3$ film) observed

in the present work is in complete agreement with the results reported by Taguchi et al. for PZT [20] and PT [21] thin films deposited by radio-frequency magnetron sputtering on platinized silicon substrates. The observation was attributed by these authors to stressed states which arises from difference in thermal expansion coefficients of the film and substrate and small grain size ($<0.5\ \mu$m). It is straight forward to suppose that the same mechanisms can be responsible for transformation of Raman spectrum reported here. Broadening of Raman peaks found for Ln-elements doped PT specimens probably indicates an increased disordering of lattice due to doping.

4.2. Room Temperature Dielectric Properties

As shown by Haertling [26], doping with donor elements (elements with higher oxidation degree than the substituted element) is compensated by cation vacancies in order to preserve electroneutrality. Donor-cation vacancy combinations are thought to be stable and so not to impede domain wall motion. Furthermore, donor doping compensates for the *p*-type conductivity inherent to lead containing perovskites through the reduction of oxygen vacancies, and this leads to higher domain wall mobility. Donor elements doped perovskite ferroelectric materials are therefore known to have higher permittivity and loss tangent than non-doped materials, and the results obtained in the present work (Fig. 6) are well in this trend. Meanwhile the increase of dielectric constant and loss tangent of doped specimens with respect to pure one can be explained in terms of contribution of domain walls oscillation the small signal dielectric properties. Observed dependence of ε' and $\tan\delta$ on the atomic number of doping element is not well understood.

The decrease in ε' and $\tan\delta$ for doping levels higher than 5 mol% may be explained in terms of the appearance (in the case of Er doping) of second pyrochlore phase, which is non-ferroelectric, or (in the case of Sm doping) to segregation effects/formation of second phases at grain boundaries which may act as pinning centres.

The previous discussion was based on the supposition that lanthanide elements ions replace lead in A-sublattice. Strictly speaking, distribution of Ln-elements between A and B sites in perovskite lattice is an object of controversy. From the calculations of cell volume and density of Ln elements doped PZT ceramics [12] it was inferred that with increasing atomic number (i.e. decreasing the ionic radii) substitution type of Ln ions changes from A- to B-type. Ln elements from La to Gd are considered to be A-site substituting donors, whereas elements from Th to Ho can substitute both A- and B-site, i.e. they are amphoteric, and elements from Er to Lu substitute Ti or Zr in B-site i.e. act as an acceptor impurities. The results obtained above show clearly that the addition of Er and Dy leads to higher dielectric constants and higher loss tangent which reflect just the opposite of what should be expected for acceptor doping elements. Therefore, it is thought that the dielectric results rather militate for Ln substitution being on A-site, i.e. donor type doping (see also the next section).

4.3. Curie Phase Transition Temperature of Pure and Ln-Elements Doped $PbTiO_3$ Films

(a) Pure $PbTiO_3$. The dielectric constant and ferroelectric phase transition temperature of ferroelectric thin films are influenced by many factors. First of all, solvent evaporation during thin film deposition and difference in thermal expansion coefficients of the film and substrate can cause the development of stress in ferroelectric thin films [27, 28]. Value and sign of the stress are strongly dependent on thin film deposition condition. Another factor affecting Curie transition temperature of the films is grain size. In particular, Shaw et al. [29] have shown that (Ba, Sr)TiO_3 (BST) thin films deposited on Si substrate undergo ferroelectric-to-paraelectric phase transition at lower temperature as compared to BST ceramics. Chattopadhyay et al. [30] investigated phase transition in nanocrystalline $PbTiO_3$, and the same effect (lowering of Curie temperature with decreasing particle size) was observed. Pronounced effect was observed when particle size was below 100 nm. It is thought that the shift of the ferroelectric transition of pure lead titanate thin film to lower temperature observed in the present work (450°C for $PbTiO_3$ thin film in comparison to 490°C of $PbTiO_3$ ceramics) may be explained both in terms of stress state and grain size (see Fig. 2). It is obvious that observed shift of Raman lines for PT and PLnT films and Curie transition temperature lowering have the same nature.

(b) Ln-Doped $PbTiO_3$. The Curie transition temperature, T_C, was found to depend on the atomic number of the Ln elements, i.e. on the ionic radii. The

results show (Figs. 8–10) that T_C decreases with the type of Ln-doping and concentration which suggest that Ln-doping leads to the weakening of the ferroelectric order, e.g. by decreasing the tetragonal distortion of the lattice (c/a) (in our previous work [31] we have demonstrated the decreasing of tetragonal distortion in sol-gel fabricated $PbTiO_3$ thin films caused by Er doping). However, the results obtained do not agree with those reported by Park et al. [12] and Tan et al. [13] on Ln-doped PZT ceramics, where T_C was found to increase with decreasing ionic radii. The results were explained in terms of the site occupancy of Ln-ions being changed from A to B with decreasing ionic radii. The results of dielectric characterization, obtained in the present work can not be explained from the same point of view. We suggest that in the case of lead titanate thin films, Ln-elements substitute lead in A-sublattice, although more investigations are needed to confirm this suggestion.

5. Conclusions

From the data of the present work next conclusions are inferred:

- Films doped with Ce, Sm, Dy and Er showed higher values of the dielectric constant. ε' and $\tan\delta$ increase with increasing atomic number of the doping elements. At low doping level (up to 5 mol%) the values of ε' and $\tan\delta$ of Sm, Dy and Er doped specimens were found to increase proportionally to doping level, x. Further doping mainly caused decrease in ε' and $\tan\delta$
- Curie transition temperature was shown to be dependent on the radius of dopant and doping level. Based on electrical measurements it is supposed that the doping elements preferentially substitute A sites in $PbTiO_3$.

Acknowledgment

The financial support of this work by the "Technologie-Stiftung Schleswig-Holstein" is gratefully acknowledged. Thanks are due to Prof. A. Neiman (Department of Inorganic Chemistry, Ural State University, Ekaterinburg) for useful discussions and to Prof. F. Tuczek and Mrs. U. Cornelissen (Institute for Inorganic Chemistry, Christian-Albrechts University, Kiel) for the help during Raman characterization.

References

1. D.L. Polla and L.F. Francis, *MRS Bull.*, **21**, 59 (1996).
2. R. Ramesh, S. Aggarwal, and O. Auciello, *Mater. Sci. Eng.*, **32**, 191 (2001).
3. W. Wersing and R. Bruchhaus, in *Handbook of Thin Film Devices*, edited by M.H. Francombe (Academic Press, New York, 2000), vol. 5, p. 168.
4. S.B. Lang and D.K. Das-Gupta, in *Handbook of Advanced Electronic and Photonic Materials and Devices*, edited by H.S. Nalwa (Academic Press, San Diego, 2001), vol. 4, p. 22.
5. M. Alguero, M.L. Calzada, and L. Pardo, *J. Mater. Res.*, **14**, 4570 (1999).
6. M. Alguero, M.L. Calzada, and L. Pardo, *J. Eur. Ceram. Soc.*, **19**, 1481 (1999).
7. S.J. Kang, J.S. Ryoo, and Y.S. Yoon, in *Ferroelectric Thin Films IV*, edited by B.A. Tuttle, S.B. Desu, R. Ramesh, and T. Shiosaki (Materials Research Society, Pittsburgh, 1995), vol. 361, p. 281.
8. T. Kamada, R. Takayama, A. Tomozawa, S. Fujii, K. Iijima, and T. Hirao, in *Ferroelectric Thin Fims V*, edited by S.B. Desu, R. Ramesh, B.A. Tuttle, R.E. Jones, and I.K. Yoo (Materials Research Society, Pittsburgh, 1996), vol. 433, p. 377.
9. Y.-K. Tseng, K.-S. Liu, J.-D. Jiang, and I.-N. Lin, *Appl. Phys. Lett.*, **72**, 3285 (1998).
10. Y.M. Kang, J.K. Ku, and S. Baik, *J. Appl. Phys.*, **78**, 2601 (1995).
11. M. Es-Souni, M. Abed, A. Piorra, S. Malinowski, and V. Zaporojtchenko, *Thin Solid Films*, **389**, 99 (2001).
12. H.-B. Park, C.Y. Park, Y.-S. Hong, K. Kim, and S.-J. Kim, *J. Am. Ceram. Soc.*, **82**, 94 (1998).
13. Q. Tan, Z. Xu, and D. Viehland, *Phyl. Mag. B*, **80**, 1585 (2000).
14. H.D. Sharma, A. Govindan, T.C. Goel, P.K.C. Pillai, and C. Pramila, *J. Mater. Sci. Lett.*, **15**, 1424 (1996).
15. C. Pramila, T.C. Goel, and P.K.C. Pillai, *J. Mater. Sci. Lett.*, **12**, 1657 (1993).
16. S.R. Shannigrahi, R.N.P. Choudhary, and H.N. Achatya, *Mater. Res. Bull.*, **34**, 1875 (1999).
17. Y. Xu, *Ferroelectric Materials* (North-Holland, Amsterdam, 1991).
18. T.J. Boyle, P.G. Clem, B.A. Tuttle, G.L. Brennecka, J.T. Dawley, M.A. Rodriguez, T.D. Dunbar, and W.F. Hammetter, *J. Mater. Res.*, **17**, 871 (2002).
19. S. Iakovlev, C.-H. Solterbeck, and M. Es-Souni, submitted to *Thin Solid Films.*
20. I. Taguchi, A. Pignolet, L. Wang, M. Proctor, F. Lévy, and P.E. Schmid, *J. Appl. Phys.*, **74**, 6625 (1993).
21. I. Taguchi, A. Pignolet, L. Wang, M. Proctor, F. Lévy, and P.E. Schmid, *J. Appl. Phys*., **73**, 394 (1993).
22. Z.C. Feng, B.S. Kwak, A. Erbil, and L.A. Boatner, *Appl. Phys. Lett.*, **64**, 2350 (1994).
23. G. Burns and B.A. Scott, *Phys. Rev.*, **B7**, 3088 (1973).
24. A.M. Glazer and S.A. Mabud, *Acta Crystallogr.*, **B34**, 1035 (1978).
25. A.L. Kholkin, S. Iakovlev, E. Fortunato, R. Martins, I. Ferreira, V. Shvartsman, and J.L. Baptista, *Key Eng. Mater.*, **230–232**, 563 (2002).

26. G.H. Haertling, *J. Am. Ceram. Soc.*, **82**, 797 (1999).
27. S.S. Sengupta, S.M. Park, D.A. Payne, and L.H. Allen, *J. Appl. Phys*., **83**, 2291 (1998).
28. G.A.C.M. Spearings, G.J.M. Dormans, W.G.J. Moors, M.J.E. Ulenaers, and P.K. Larsen, *J. Appl. Phys*., **78**, 1926 (1995).
29. T.M. Shaw, Z. Suo, M. Huang, E. Liniger, R.B. Laibowitz, and J.D. Baniecki, *Appl. Phys. Lett.*, **75**, 2129 (1999).
30. S. Chattopadhyay, P. Ayyub, V.R. Palkar, and M. Multani, *Phys. Rev. B*, **52**, 13177 (1995).
31. S. Iakovlev, M. Avdeev, C.-H. Solterbeck, and M. Es-Souni, *Phys. Stat. Sol. (a)*, **198**, 121 (2003).